Research Square

Preprints are preliminary reports that have not undergone peer review.
They should not be considered conclusive, used to inform clinical practice,
or referenced by the media as validated information.

Assessing ecological risk in the riparian zone of the Punatsangchhu river basin, Bhutan: Prioritizing White-bellied Heron habitat

Asish Subba

subbaashish173@gmail.com

Nalanda University https://orcid.org/0009-0004-3820-6677

Satyanarayan Shashtri

Nalanda University

Research Article

Keywords: Riparian zone Management, Bhutan, Punatsangchhu river basin, Ecological risk assessment, Remote Sensing, GIS

Posted Date: August 25th, 2026

DOI: https://doi.org/10.21203/rs.3.rs-10591963/v1

License: This work is licensed under a Creative Commons Attribution 4.0 International License.
Read Full License

Additional Declarations: The authors declare no competing interests.

Assessing ecological risk in the riparian zone of the Punatsangchhu river basin, Bhutan: Prioritizing White-bellied Heron habitat

Asish Subba[1,*], Satyanarayan Shashtri[1]

[1]School of Ecology and Environment Studies, Nalanda University, Rajgir, Bihar, India

[*]Corresponding email: subbaashish173@gmail.com

Abstract

The riparian zone is the most biodiverse ecoregion, which provides essential functions and services to humankind. The riparian zone is significantly affected by human activities worldwide. This study integrated remote sensing, geographic information system, and machine learning algorithms to predict the risk vulnerability in the riparian zone of the Punatsangchhu River Basin. The current study used 11 predictors, including land use and land cover, geomorphology, and others, to assess riparian zone risk. The model's overall predictive accuracy was good, with RF (AUC = 0.97) outperforming SVM (AUC = 0.94).

Land use and land cover, and geomorphology were the most influential predictors of the riparian zone risk vulnerability based on information gain ratio (InGR). The findings show that very high risk areas constitute 11% and 14%, respectively, according to SVM and RF. The result also revealed that very high and high risk areas within the riparian zone were dominant in the middle, lower, and upper regions of the Punatsangchhu River Basin. The low-risk class is the most prominent in the riparian zone, with 50% and 49% by SVM and RF, respectively.

These findings provide critical information to competent authorities for formulating and implementing risk response measures to protect the riparian zone. It helps prioritize high and very high risk areas for restoration and remediation, and regularized buffer zoning to support future hydropower development. Moreover, the high risk areas coinciding with the habitat of the White-bellied Heron could be prioritized for restoration to aid conservation. Thus, this makes the present study critical for supporting the planning and management of the riparian zone and river basin as a whole.

Keywords: Riparian zone Management, Bhutan, Punatsangchhu river basin, Ecological risk assessment, Remote Sensing, GIS

Introduction

Freshwaters are one of the most altered and threatened ecosystems in the world (Millennium Ecosystem Assessment (MEA), 2005). The recent Planetary Health Check (PHC) report found that humans have exceeded the safe operating space of Earth for freshwater use (Kitzmann et al., 2025). As a result, numerous studies have reported reductions in water quality, ecosystem services, and freshwater ecosystems (MEA, 2005; Whitehead et al., 2009; Jones et al., 2010; Dodds et al., 2013). Climate change, alterations in hydrological flows, land-use change, chemical effluents, and aquatic invasive species are the major drivers reshaping freshwater systems (Carpenter et al., 2011). The global assessment report of Intergovernmental Science-Policy Platform on Biodiversity and Ecosystem Services (IPBES) reported that the global species extinction is accelerating at an unprecedented rate worldwide (IPBES, 2019).

In such conditions, areas with more stable temperatures and higher water availability, and the potential to buffer against environmental extremes and climate change, are of utmost importance (Ashcroft, 2010). In this context, Zhang et al. (2023) elucidated that riparian zones serve as suitable habitats, creating moist microenvironments that are habitable for woody plant species under a changing climate. The riparian zone is the transitional ecotone between terrestrial and freshwater systems, shaped by fluvial geomorphological processes and delineated spatially using GIS techniques (Gregory et al., 1991; Naiman & Décamps, 1997; Johansen & Phinn, 2006). The riparian zone is recognized as the 15th terrestrial biome (Burger et al., 2010; Maraseni & Mitchell, 2016; Majumdar & Avishek, 2023). They occupy a small ecological space, yet it is one of the most biodiverse ecosystems in the world (Gregory et al., 1991).

Accordingly, riparian vegetation plays an extremely important role in regulating soil erosion, channel stability, water quality, and supporting biodiversity (Gregory et al., 1991). Numerous studies examined the role of riparian vegetation in filtering and removing dissolved nutrients such as nitrogen, phosphorus, and toxins (Correll et al., 1992; Narumalani et al., 1997; Toole et al., 2018). For instance, Correll et al. (1992) reported that riparian vegetation next to agricultural fields was effective in removing 80% of the nitrate and 85% of the total phosphorus during surface land flooding, and about 85% of the nitrate in sub-surface groundwater drainage from the cropland.

From the very beginning of civilization, riparian zones around the world have been leveraged to build major industrial zones and urban settlements due to the abundant natural resources and low transportation costs. For instance, significant rivers such as the Congo in Africa, the Danube in Europe, the Great Lakes in North America, and the Murray in Australia have developed their riparian fringes into urban centres (Funk et al., 2019; Garcin et al., 2022; Grafton et al., 2014; Zhu et al., 2025). Presently, the riparian zone is the focus of hydropower dam constructions in the Himalayan landscapes (He et al., 2024; Kaintura et al., 2024; Li et al., 2024).

Despite the benefits of riparian zones for human well-being, they are becoming vulnerable due to rapid industrialization, urbanization, and agricultural expansion (Zhu et al., 2025). Major rivers and associated riparian zones are facing significant environmental challenges (Naiman & Décamps, 1997; Zhu et al., 2025). For instance, the Rhine River faces the pressing issue of industrial pollution and urban development. Similarly, the Ganges River Basin is facing severe water pollution, declining riparian wetlands, and excessive exploitation of water resources (Zhu et al., 2025). Additionally, due to high population density, rapid urbanization, and pollution, the ecological degradation in riparian areas has been exacerbated. As a result, riparian vegetation such as cottonwood (*Populus fremontii*) and willow (*Salix exigua*) is disappearing worldwide (Hultine et al., 2010). Due to these, the original ecosystem services of riparian zones, such as landscape functions and carbon sequestration, have been severely compromised (Burger et al., 2010; Maraseni & Mitchell, 2016).

At the same time, studies in Bhutan focusing on the Punatsangchhu River Basin have also reported significant changes in land use and land cover due to hydropower dam construction (Wangdi, 2014). The changes are significantly associated with the presence of the White-bellied Heron (*Ardea insignis*), indicating disturbance caused by dam construction in their habitats (Wangdi, 2014). The growing conflict between resource development and ecological protection in the riparian zones of the Punatsangchhu River Basin highlights the urgent need for sustainable management strategies. However, ecological risk assessment studies focusing on the riparian zone are limited (Zhu et al., 2025). Furthermore, studies assessing ecological risk in the riparian zone rely mostly on ERA models and GIS techniques (United States Environmental Protection Agency (USEPA), 1998). Therefore, it is essential to integrate geospatial and machine learning techniques to more accurately assess ecological risk and effectively target conservation and protection of the riparian zone.

Recently, studies using remote sensing and GIS have attracted the researcher's attention. In particular, remote sensing and GIS are increasingly applied to assess ecological risk and ecosystem vulnerability. However, these studies assessing ecological risk have focused more on wetland ecosystems (Islam et al., 2021a), coastal zones, river basins, protected areas, administrative districts, urban agglomerations, and transboundary river basins (Wang et al., 2020; Cui et al., 2022). Only a limited number of studies have focused on the ecological risk assessment of riparian zones. For instance, Zhu et al. (2025) evaluated the ecological risk in the riparian zone of Jiangsu province along the Yangtze River using multiple risk drivers. Furthermore, riparian zone mapping is a prerequisite for assessing ecological risk in the riparian zone. High-resolution satellite imagery offers a significant advantage for monitoring riparian zones compared to traditional field-based methods. However, mapping the actual extent of riparian zones remains challenging due to their fuzzy boundaries (Betz et al., 2018). Mostly, studies used a fixed buffer around the river channel to estimate the riparian zone extent, but this method does not accurately reflect the true extent of the riparian zone. The literature suggests that integrating remote sensing and GIS with fuzzy logic

can yield reliable, accurate estimates of the riparian zone (Clerici et al., 2013, 2014; Weissteiner et al., 2016; Betz et al., 2018). Furthermore, machine learning techniques can improve the accuracy of the riparian zones mapping (Salo & Theobald, 2016).

In contrast to the delineation of the riparian zone, a major methodological gap persists in studies of riparian zone ecological risk assessment. Although studies have used remote sensing and GIS in the riparian zone risk assessment. Their integration with machine learning algorithms is limited in riparian zone risk assessment. Notably, Islam et al. (2021a) employed machine learning to assess the risk in the riparian wetland, but specific ecological risk assessment in the riparian zone is limited. This study will address this methodological gap by integrating remote Sensing, GIS, and machine learning algorithms to assess the ecological risk in the riparian zone of the Punatsangchhu River.

Despite growing pressures on Bhutan's rivers from land-use change driven by hydropower construction (Wangdi, 2014). There is a geographical gap present in Bhutan's river basin. To date, the ecological risk assessment of Bhutan's river basin has not been explored. Most studies focus on documenting the macroinvertebrate diversity and plant species composition (Lhundup & Dorji, 2018; Jamtsho et al., 2021; Lungten et al., 2023; Gurung et al., 2024; Jamtsho et al., 2024; Thukten, 2024). Moreover, to date, Bhutan has not mapped the extent and distribution of the riparian zone, which is an initial requirement for ecological risk assessment studies. In this context, this study will employ variable-width buffering to estimate the riparian zone extent and assess the ecological risk within the riparian zones of the Punatsangchhu River Basin. Thus, this dissertation fills the geographical gap by assessing the ecological risk in the Punatsangchhu River Basin. Thus, this paper provides an explicit assessment of ecological risk in the riparian zone, offering critical information for the conservation and monitoring of ecological risks in the riparian areas of the Punatsangchhu River Basin.

Research Objectives

The specific research objectives of this study are;

- To **demarcate** the riparian zone extent using a variable-width buffering technique in the Punatsangchhu River Basin.
- To **evaluate** the key environmental variables influencing the ecological risk of the riparian zone.
- To **compare** the performance of machine learning algorithms in the riparian zone ecological risk model.
- To **analyze** the spatial distribution of ecological risk of the riparian zone in the Punatsangchhu River basin.
- To **provide** information on the riparian landscape planning, and support identifying critical areas for ecological protection.

Materials and methods

Study area

The Figure 1 shows the study area, the Punatsangchhu River Basin. It is situated in the western region of Bhutan, precisely at longitudes 89.03 E to 90.02 E and latitudes 27.34 N to 28.09 N. It is located at elevations ranging from 98 m above sea level to 7057 m above sea level (the elevation values are derived from the SRTM DEM used in this study). It comprises 5 districts of Bhutan, Gasa in the upper region of the basin, Punakha and Wangdue Phodrang in the central region, and Tsirang and Dagana in the southern part. The Punatsangchhu River Basin is characterized by heavy rainfall at lower elevations and low rainfall at higher elevations. The average annual rainfall is 110 mm. The common geomorphological features of the study area include highly dissected hills and valleys, moderately dissected hills and valleys in the central region, glacier landforms in high-elevation mountains, and alluvial fans at lower elevations.

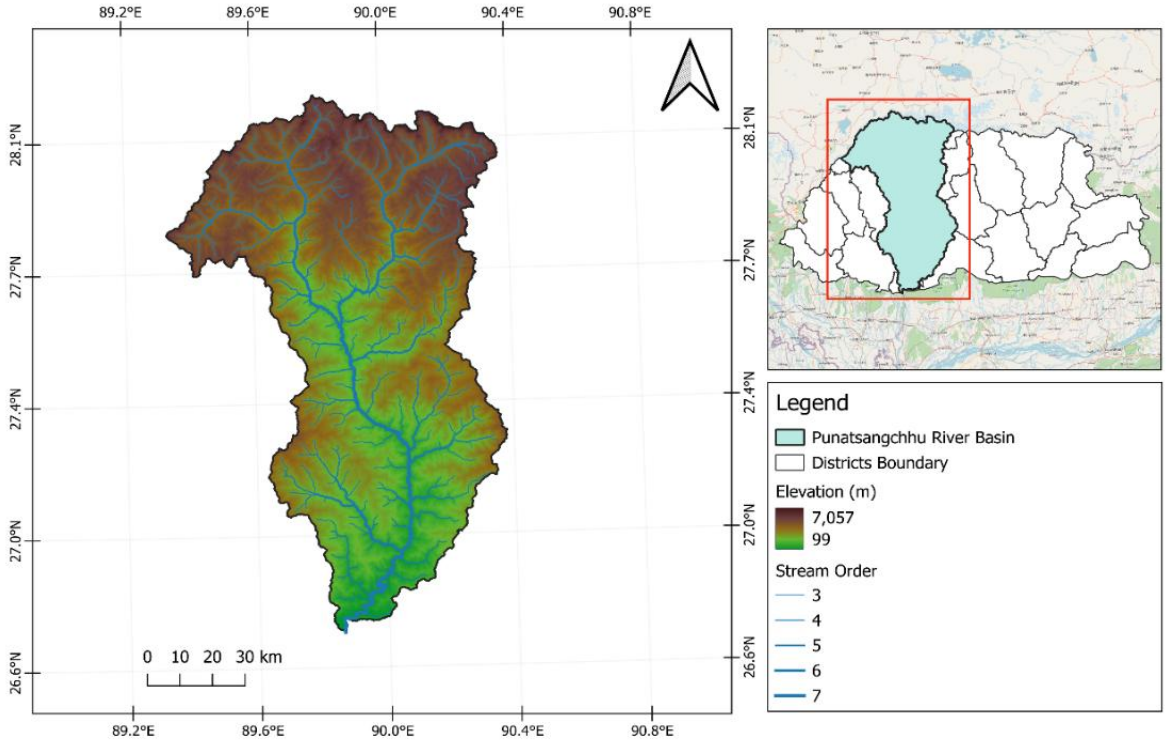


Figure 1: Map showing the location of the Punatsangchhu River Basin.

Data Acquisition

Selection and generation of indicators for riparian zone risk assessment

Riparian zone risk characterization is influenced by distinct sets of biophysical and anthropogenic factors (Zhu et al., 2025). To account for this diversity, a set of common environmental indicators of riparian zone risk was selected based on the available literature. In this study, a total of 11 indicators were selected and standardized to a common coordinate reference system (CRS) and

spatial resolution to ensure consistency. Therefore, all raster data layers were reprojected to UTM zone 45N and resampled to a 30 m spatial resolution. Analysis
In this study, an elevation map was derived from the Shuttle Radar Topography Mission (SRTM) with a 30 m resolution. The SRTM DEM was downloaded from the openly accessible United States Geological Survey data portal (https://earthexplorer.usgs.gov/). The slope is also a relevant biophysical factor for the riparian zone risk assessment. It determines the flow direction and stability of the riparian zone and influences the geophysical events such as landslides, floods, and erosion. In this study, a slope map was derived from the SRTM DEM with a 30 m resolution.

Geology, Geomorphology, and Soil

Geological features influence hydrogeological characteristics, and hence, geological data is considered an important parameter in risk assessment in this study. In this study, geology data was downloaded from the National Spatial Data Infrastructure (NSDI) database (https://nsdi.systems.gov.bt/). This database provides basic geospatial data for Bhutan, including geological maps, administrative data, and other ancillary data. Then, the acquired geology data was processed in a GIS platform (QGIS version 3.4) to derive geological classes.

In this study, geomorphology is considered an influential geophysical factor controlling river dynamics, bank stabilization, and sediment deposition, indicating strong risk indicators for the riparian zone. Therefore, the geomorphological map was prepared by visual interpretation of multiple thematic map layers, including LULC, satellite imagery (Landsat 8 OLI and Sentinel-2), and DEM-derived parameters, using digitization. The geomorphological map was prepared at a scale of 1:50,000 following the Indian Space Research Organization (ISRO) manual (ISRO, 2010). The Indian Space Research Organization's level 2 classification was used in the current study.

Soil characteristics are also a crucial indicator in riparian zone risk assessment, as they influence surface runoff and nutrient transfer. It also influences hydrometeorological events, such as rainfall-induced landslides and flash floods. In this study, soil data was downloaded from the Food and Agriculture Organization (FAO) data portal (https://www.fao.org/soils-portal/en/). Then, the soil data obtained from the portal is processed in QGIS to derive soil class classification.

Normalized Difference Vegetation Index

The Normalized Difference Vegetation Index (NDVI) is a crucial factor in riparian zone risk assessment, as it reflects vegetation health and ecosystem stability. In this study, NDVI was extracted from Landsat 8 Operational Land Imager (OLI) imagery. The following equation was used to compute NDVI (Equation 1) (Fu & Burgher, 2015). The Landsat 8 OLI data was downloaded from the United States Geological Survey (USGS) data portal (https://earthexplorer.usgs.gov/).

$$\mathrm{NDVI} = \frac{\mathrm{NIR} - \mathrm{RED}}{\mathrm{NIR} + \mathrm{RED}} = \frac{\text{band 5} - \text{band 4}}{\text{band 5} + \text{band 4}} \quad \text{(Equation 1)}$$

Where the NIR refers to the near infrared range of electromagnetic radiation (EMR), and it is represented by band 5 of Landsat 8 OLI. The RED refers to the red range of the visible spectrum of light, and corresponds to the 4th band of Landsat 8 OLI. The NDVI values range from -1 to +1 (Fu & Burgher, 2015). Positive values closer to 1 indicate green and healthy vegetation, while values close to -1 indicate barren land, waterbodies, or a built-up area (Fu & Burgher, 2015).

Normalized Difference Moisture Index

The Normalized Difference Moisture Index (NDMI) reflects water level in vegetation and directly influences vegetation health and ecosystem stability. In this study, NDMI was extracted from Landsat 8 OLI imagery (Bottaro et al., 2025). The following equation was used to compute NDMI (Equation 2).

$$\text{NDMI} = \frac{\text{NIR} - \text{SWIR1}}{\text{NIR} + \text{SWIR1}} = \frac{band\ 5 - band\ 6}{band\ 5 + band\ 6} \quad \text{(Equation 2)}$$

Where the NIR refers to the near infrared range of electromagnetic radiation, and it is represented by band 5 of Landsat 8 OLI. While SWIR1 refers to the short-wave infrared of the electromagnetic radiation, and corresponds to the 6th band of Landsat 8 OLI. The NDMI values range from -1 to +1 (Bottaro et al., 2025). Positive values closer to 1 indicate vegetation water content, while values close to -1 indicate no direct connection and represent barren land and drought conditions (Bottaro et al., 2025).

Normalized Difference Built-up Index

The Normalized Difference Built-up Index (NDBI) is a crucial factor in riparian zone risk assessment, as it reflects urbanization and population concentration in the riparian corridors. Zhu et al. (2025) found that built-up area is the most influential factor in the riparian zone risk assessment. In this study, NDBI was extracted from Landsat 8 OLI imagery. The following equation was used to compute NDBI (Equation 3) (Bhatti & Tripathi, 2014; Florim et al., 2021).

$$\text{NDBI} = \frac{\text{SWIR1} - \text{NIR}}{\text{SWIR} + \text{NIR}} = \frac{band\ 6 - band\ 5}{band\ 6 + band\ 5} \quad \text{(Equation 3)}$$

Where the SWIR1 refers to the short-wave infrared range of electromagnetic radiation, and it is represented by band 6 of Landsat 8 OLI. NIR refers to the near-infrared, which corresponds to the 5th band of Landsat 8 OLI. The NDBI values range from -1 to +1 (Florim et al., 2021). Positive values closer to 1 indicate high urban development, while values close to 0 indicate low urban development (Bhatti & Tripathi, 2014).

Distance to River

The distance to river is an important indicator of the riparian zone risk assessment. It influences riparian vegetation through hydrodynamic conditions such as flooding and bank erosion (Islam et al., 2021a). Therefore, the distance to the river has been considered the relevant indicator of

riparian zone risk assessment. The Euclidean distance method was employed to prepare distance to river maps, following Islam et al. (2021a).

Land Use and Land Cover

The land use and land cover map is an important anthropogenic indicator of the riparian zone risk assessment. It determines habitat alterations and land use practices in the riparian zone (Olokeogun & Kumar, 2020; Olokeogun & Kumar, 2022). In this study, land-use and land-cover data was downloaded from the Environmental Systems Research Institute (ESRI) data portal (https://livingatlas.arcgis.com/landcover/).

Precipitation

Rainfall is also an important bioclimatic indicator of riparian zone risk assessment. It determines drought conditions and influences hydrometeorological hazards, such as rainfall-induced landslides and flash floods in the riparian zone (Islam et al., 2021a). Therefore, precipitation is considered an influential indicator of the riparian zone risk assessment. In this study, rainfall data was downloaded from the Center for Hydrometeorology and Remote Sensing website (CHRS) data portal (https://chrsdata.eng.uci.edu/).

Information Gain Ratio (InGR) to assess the factors influencing the riparian zone risk modeling

Information gain ratio (InGR) is a feature selection method useful for selecting the high ranking predictors before modeling (Islam et al., 2021a). Thus, following the standard modeling procedure, the information gain ratio (InGR) was used to select the most relevant parameters for riparian zone risk assessment, as described by Islam et al. (2021a). The higher the InGR value, the greater the influence of drivers on riparian zone degradation and fragmentation. Thus, in this study, riparian indicators with high InGR values are retained only for model building. The InGR technique is widely used due to its simplicity and efficacy. In this study, the following equation was used to assess the factors influencing riparian zone risk assessment (Equation 4).

$$\text{Gain ratio (y, M)} = \frac{\text{Entropy }(M) - \sum_{1}^{n} \sum_{1=i}^{n} \frac{|M_i|}{|M|} \text{ Entropy }(M_i)}{-\sum_{1=1}^{n} \frac{|M_i|}{|M|} \log \frac{|M_i|}{|M|}} \qquad \text{(Equation 4)}$$

Where the attribute y belongs to a training point M with subsets M_i = 1, 2, 3, …n

Catchment delineation

Catchment or basin delineation is the foundation for the riparian zone risk assessment. In this study, a Shuttle Radar Topography Mission (SRTM) Digital Elevation Model (DEM) was used to delineate the catchment of the Punatsangchhu River. As SRTM DEM has a coarse resolution of 30m, it contains sinks or depressions due to artificial pits, vegetation, or noise. These could hamper for calculating flow direction and flow accumulation, and they need to be corrected before the stream network derivation. Wang & Liu (2007) employed a sink-filling method to create a "hydrologically correct" DEM without depressions.

This is a common method to overcome this problem, and after the fill sink, the flow accumulation was calculated using the deterministic 8 method. Afterward, the channel was extracted from the flow accumulation grid, where the initiation threshold was selected based on digitized channel heads. In this study, sink filling and the computation of the flow accumulation grid and the channel network were conducted in SAGA GIS, a QGIS plugin.

Riparian zone mapping

Mapping the riparian zone is a prerequisite for the risk assessment. In this study, variable-width buffering was applied to stream data to delineate the riparian zone in the Punatsangchhu River Basin. The delineation of the riparian zone's exact extent is not straightforward, and it remains a matter of debate due to its indeterminate outer boundary. Several methods have been employed to demarcate the riparian zone, including variable-width buffering, fixed-width buffering, fuzzy logic theory, and machine learning as well (Clerici et al., 2013, 2014; Weissteiner et al., 2016; Betz et al., 2018; Salo & Theobald, 2016). However, variable-width buffering based on stream strahler order was used in this study for riparian zone delineation.

In the present study, stream strahler orders above 3 are included only as units of analysis, as they represent perennial streams and improve visualization of the riparian zone (Strahler orders 3-7). The following options for stream variable buffering were implemented in this study: 1) buffer width of 50 m was applied for 3^{rd} order streams, 2) 100 m was applied for 4^{th} order streams, 3) 200 m was applied for 5^{th} order streams, 4) 300 m was applied for 6^{th} order streams, and 5) buffer width of 500 m was applied for 7^{th} order streams (Apan et al., 2002). The specific buffer width used in this study was chosen based on a literature review and knowledge of the study areas, following Apan et al. (2002).

Riparian zone risk assessment using machine learning algorithms

Random Forest

Random Forest (RF) is a supervised machine learning algorithm primarily used for regression and classification (Lesmeister, 2017). It is a widely used machine learning algorithm that has recently been applied to riparian zone classification (Salo & Theobald, 2016). In the present study, RF has been used to assess the risk in the riparian zone. The RF algorithm is an ensemble classifier that builds multiple decision trees and averages their outputs for robust prediction and classification (Lesmeister, 2017). It is recommended to grow multiple trees to build a robust model.

Support Vector Machine

Support Vector Machine (SVM) is one of the most widely used supervised machine learning algorithm (Lesmeister, 2017). It is widely used for classification, pattern recognition, and regression across many fields, including statistics, finance, environmental sciences, and risk assessment. In this study, SVM is used to predict riparian-zone risk. The model can be expressed by the following equation (Equation 5).

$$z = f(y) = \sum_{i=1}^{n} w_i \phi_i = w\phi(y) \quad \text{(Equation 5)}$$

Where the model output refers to the linear part of *P,* (). The converter is modeled by a nonlinear model. The SVM model is represented by the following equation (Equation 5).

$$z = f(y) = \left\{\sum_{i=1}^{l} w_i K\ (Y_i, Y\right\} - c \quad \text{(Equation 6)}$$

Accordingly, while the Y_i and Y represent the data vector for network learning and the independent vector, respectively. The model parameters are determined by maximizing the objective function.

Riparian zone risk modeling technique

For supervised machine learning algorithms, binary labelled data is required to train and test the model. In this regard, the present study used the landscape fragmentation map (generated with the Landscape Fragmentation Tool (LFT v2.0), an ArcGIS extension) to prepare the inventories of the riparian zone risk model. The fragmentation map contains 6 classes, such as 1) Patch, 2) Edge, 3) Perforated, 4) Small core, 5) Medium core, and 6) Large core. In this study, the patch and edge are the most detached and fragmented parts of the riparian zone and have a very high risk of conversion to other land uses, while the large core has a very low or no risk of conversion (Islam et al., 2021a). The fragmentation class was used solely to derive the training and testing data in the current study. It is not used as a spatial predictor of the riparian zone risk assessment. Thus, the resulting outputs, such as maps and tables, are not discussed in the main results, and they are provided as supplementary materials (Supplementary file Figure 20, Table 2).

Therefore, following the logic reported by Islam et al. (2021a), we randomly selected 225 points from the patch and edge fragmentation class and assigned them a value of 1, and 225 points from the large core fragmentation class, assigning them a value of 0. In the present study, 0 indicates non-risk areas, and 1 indicates risk areas for training and testing machine learning algorithms. A total of 450 data points were collected, and the dataset was split into training (80%) and test (20%) sets. The training points, which contain both 0 and 1 values, were used to extract data from 11 riparian zone drivers. Based on the 80% of the training dataset, we developed riparian zone risk assessment models using machine learning algorithms. Then, the remaining 20% validation datasets were used to extract predicted data from the riparian zone risk assessment models, which were then used to validate the models (Section 3.4). Due to the large size of the complete dataset used to train the riparian zone risk model, a preview of the data used in this study is provided as supplementary material (Supplementary file, Table 2). The full dataset is available upon request from the corresponding author.

Model validation

In the present study, the riparian zone risk assessment models were validated using a commonly used evaluation metric, namely the area under the curve (AUC) of the receiver operating characteristic (ROC) curve. The remaining test dataset (20%) was used to construct the ROC curve. To construct the ROC curve, sensitivity is plotted on the x-axis and specificity on the y-

axis. The AUC value of the ROC curve ranges from 0 to 1. AUC values less than 0.5 indicate poor model performance, and AUC values between 0.5 and 0.7 indicate fair model performance. Models with AUC values between 0.7 and 0.9 are considered good, and an AUC value greater than 0.9 indicates high model performance. Sensitivity refers to the model's ability to correctly predict true positives, and specificity refers to its ability to correctly predict true negatives. The sensitivity and specificity were calculated following the equations (Equation 7 and Equation 8).

$$\text{Sensitivity} = \frac{a}{a + c} \quad \text{(Equation 7)}$$

$$\text{Specificity} = \frac{d}{b+d} \quad \text{(Equation 8)}$$

where *a* refers to the TP (true positives are correctly classified risk pixels), *b* refers to the FP (false positives are non-risk pixels classified as risk pixels), *c* indicates the FN (false negatives are risk pixels classified as non-risk pixels), and *d* represents the TN (true negatives are correctly classified non-risk pixels).

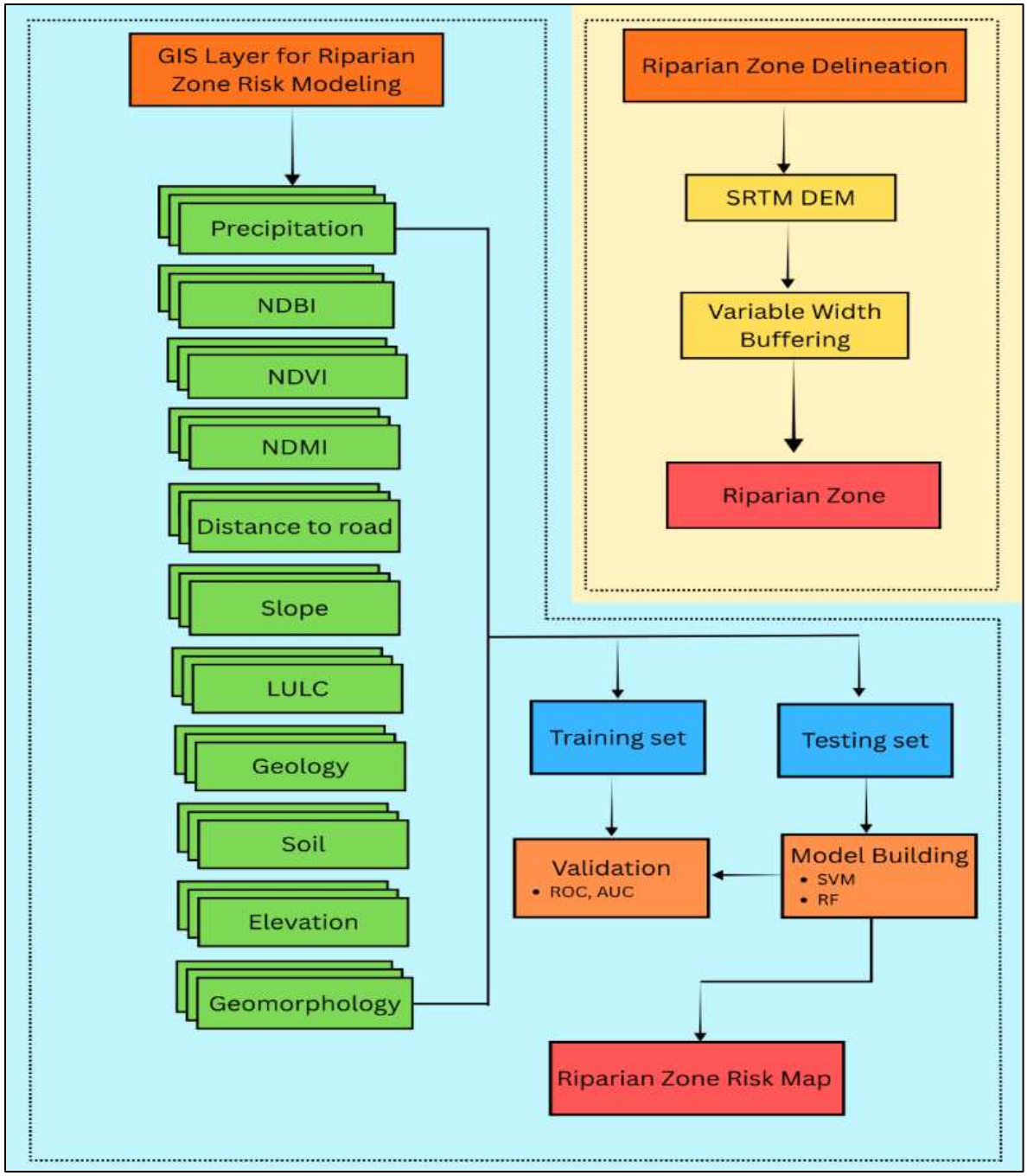


Figure 2: Overall workflow diagram for riparian zone risk assessment

Results and discussion

Results

Catchment and riparian zone delineation

The delineated catchment of the Punatsangchhu River Basin and its tributaries is presented in Figure 3. The catchment has a total area of 9677.74 km². The riparian zone generated from variable-width buffering of stream data is shown in Figure 4. The total area of the delineated riparian zone is 865.445 km².

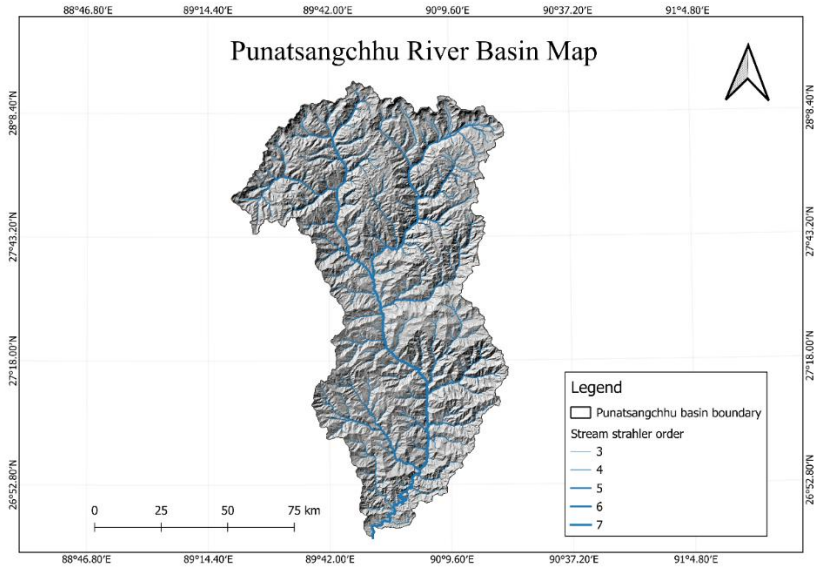


Figure 3: The map shows the delineated Punatsangchhu River Basin and strahler stream order.

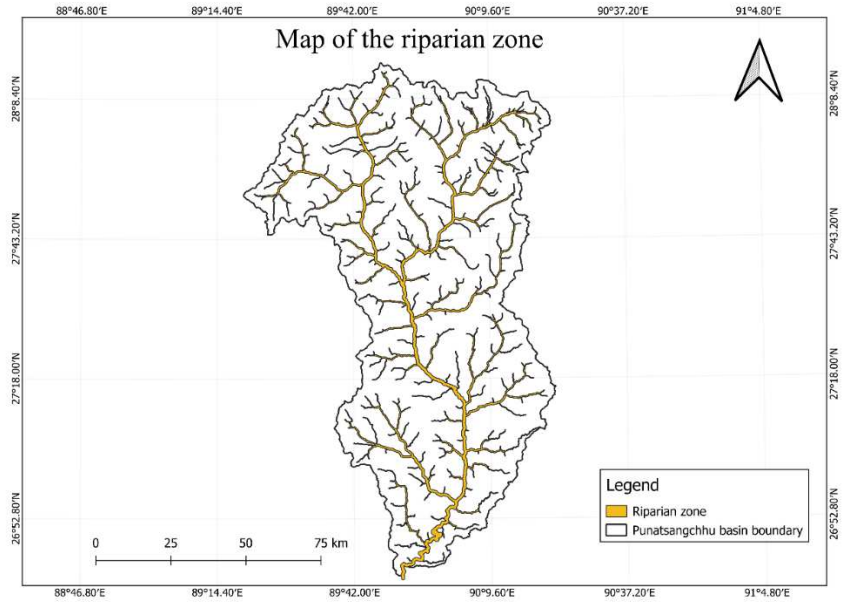


Figure 4: The map shows the riparian zone along the Punatsangchhu River.

Factors influencing the riparian zones risk assessment

Elevation and Slope

The elevation map of the riparian zones in the Punatsangchhu River Basin is presented in Figure 5a. The elevation in the riparian zone of the Punatsangchhu River Basin ranges from 98 m to 5154 m. It is clearly visible on the map that the lower region of the study area is characterized by low elevation values (green), while the upper region shows higher elevation values (red). The slope map of the riparian zones in the Punatsangchhu River Basin is presented in Figure 5b. The slope of the riparian zone in the Punatsangchhu River Basin ranges from 0.007º to 78.79º. From the map below, the blue areas show low slope values, usually flat or plain areas, and the red areas show hills and cliffs.

Land Use and Land Cover (LULC)

The land-use and land-cover (LULC) map of the riparian zones in the Punatsangchhu River Basin is shown in Figure 5c. The riparian zone in the Punatsangchhu River Basin encompasses various LULC classes, including water, trees, flooded vegetation, crops, built-up areas, bare ground, snow/ice, and rangelands. The trees represent the highest percentage of the LULC class at 68.07 %, followed by rangelands at 23.03 % and bare ground at 3.30 %. The details of LULC classes and their corresponding areas are presented in Table 1.

Table 1: Details of the LULC classes and their area.

LULC Code	LULC Class	Area (Km²)	Area (%)
1	Water	25.741	2.97%
2	Trees	588.998	68.07%
4	Flooded vegetation	0.048	0.01%
5	Crops	8.648	1.00%
7	Built Area	10.996	1.27%
8	Bare ground	28.55	3.30%
9	Snow/Ice	3.048	0.35%
11	Rangelands	199.288	23.03%
Total		**865.445**	**100.00%**

Normalized Difference Vegetation Index

The NDVI map of the riparian zones in the Punatsangchhu River Basin is presented in Figure 5d. The NDVI values in the riparian zone of the Punatsangchhu River Basin range between -0.255 and 0.958. High NDVI values reflect healthy, green vegetation, while low NDVI values indicate stressed vegetation (Florim et al., 2021). NDVI values in the negative range indicate barren lands and built-up areas within the riparian zone of the Punatsangchhu River Basin (Fu & Burgher, 2015).

Normalized Difference Moisture Index

The NDMI map of the riparian zones in the Punatsangchhu River Basin is presented in Figure 5e. The NDMI values in the riparian zone of the Punatsangchhu River Basin range between -0.32 and 0.584. High NDMI values reflect higher moisture content in vegetation, while low NDMI values indicate low moisture content or water-stressed vegetation (Bottaro et al., 2025). NDMI values in the negative range indicate low moisture content and likely barren land and non-vegetated areas within the riparian zone of the Punatsangchhu River Basin (Bottaro et al., 2025).

Normalized Difference Built-up Index

The NDBI map of the riparian zones in the Punatsangchhu River Basin is presented in Figure 5f. The NDBI values in the riparian zone of the Punatsangchhu River Basin range between -0.584 and 0.327. The green color on the map indicates low NDBI values, while red indicates high NDBI values. High NBVI values reflect higher built-up areas, while low NDBI values indicate low built-up intensity (Bhatti & Tripathi, 2014). NDBI values in the negative range indicate barren land and water bodies within the riparian zone of the Punatsangchhu River Basin (Florim et al., 2021).

Geology

The geology map of the riparian zones in the Punatsangchhu River Basin is presented in Figure 5g. The riparian zone in the Punatsangchhu River Basin comprises of various geology class such as Greater Himalayan metasedimentary unit, Greater Himalayan lower metasedimentary unit, Greater Himalayan upper metasedimentary unit, Greater Himalayan orthogneiss unit, Greater Himalayan undifferentiated, Cretaceous (undifferentiated), Daling Formation, Chekha Formation, Paleozoic (undifferentiated), Leucogranite, Tethyan Himalayan (undifferentiated), Triassic–Jurassic (undifferentiated), and Siwalik Group (Middle member). The leucogranite class is dominant in the riparian zone, accounting for 51.03%, followed by the Greater Himalayan upper metasedimentary unit (14.73%) and the Greater Himalayan orthogneiss unit (8.40%). The details of the various geology classes, their corresponding areas, and percentages are shown in Table 2. The Greater Himalayan lower metasedimentary unit consists of 6.5–7 km of upper amphibolite-to-granulite-facies paragneiss with rare quartzite layers in western Bhutan (Mcquarrie et al., 2013). These rock units are highly fractured and susceptible to mass wasting and debris flow. The Greater Himalayan Upper Metasedimentary Unit consists of medium- to thick-bedded, micaceous quartzite interlayered with paragneiss and schist (Mcquarrie et al., 2013). These rock units are characterized by weak planes that are prone to landslides in the riparian zone.

Table 2: Details of the geology class and its areas and percentages.

Geology Code	Geology Clas	Area (Km²)	Percentage (%)
pCd	Daling Formation	18.042	2.08%
Pzu	Paleozoic, undifferentiated	13.211	1.53%
Tgr	Leucogranite	441.678	51.03%

Tsm	Siwalik Group (Middle member)	57.56	6.65%
GHlml	Greater Himalayan lower metasedimentary unit	36.618	4.23%
GHhm	Greater Himalayan metasedimentary unit	6.259	0.72%
GHml	Greater Himalayan (undifferentiated)	43.511	5.03%
Tr-Jru	Triassic–Jurassic (undifferentiated)	11.627	1.34%
THu	Tethyan Himalayan (undifferentiated)	1.598	0.18%
Ku	Cretaceous, undifferentiated	5.589	0.65%
GHlo	Greater Himalayan orthogneiss unit	72.686	8.40%
Pzc	Chekha Formation	29.569	3.42%
GHlmu	Greater Himalayan upper metasedimentary unit	127.501	14.73%
Total		**865.445**	**100.00%**

Geomorphology

The geomorphology map of the riparian zones in the Punatsangchhu River Basin is presented in Figure 5h. The riparian zone in the Punatsangchhu River Basin is classified as level 2 origin and encompasses five soil types: Alluvial plain, Glacier Valleys, Rivers, Low Dissected Hills and Valleys, and Moderately Dissected Hills and Valleys. Alluvial plains are low-lying landforms formed by fluvial processes, such as sediment deposition (ISRO, 2010). These landforms are fertile and flat, attracting agricultural activities and human settlements, which can exacerbate ecological risk in the riparian zone. Glacier valleys are landforms created by glacier processes and are the source of downstream river flow (ISRO, 2010). These landforms often pose a risk of Glacier Lake Outburst Floods (GLOFs), increasing ecological vulnerability in the riparian zone.

Soil

The soil map of the riparian zones in the Punatsangchhu River Basin is presented in Figure 5f. The riparian zone in the Punatsangchhu River Basin encompasses six soil types, including Gleysols, Orthic Acrisols, Dystric Nitosols, Dystric Cambisols, Dystric Regosols, and Lithosols. The Orthic Acrisols (51.66%) is the most prominent soil type in the riparian zone of the Punatsangchhu River Basin. The Lithosols follow with 24.48%, and Dystric Cambisols with 19.54 %. Further details of all soil types, their areas, and percentages are given in Table 3. Gleysols are a type of soil characterized by hydric waterlogged conditions, which can increase the risk of flooding in the riparian zone (FAO, 1974). Lithosols are a type of soil represented by hard rock, which can hinder infiltration and increase surface runoffs, causing floods in the riparian zone (FAO, 1974).

Table 3: Details of six soil type, their areas, and percentages.

FAO-UNESCO Soil Code	Soil Class	Area (Km²)	Percentage (%)
GL	Gleysols	28.728	3.32%
Ao	Orthic Acrisols	447.091	51.66%
Nd	Dystric Nitosols	6.517	0.75%
Bd	Dystric Cambisols	169.107	19.54%

Rd	Dystric Regosols	2.121	0.25%
I	Lithosols	211.884	24.48%
Total		**865.445**	**100.00%**

Distance to River

The distance to the river map of riparian zones in the Punatsangchhu River Basin is presented in Figure 5j. The euclidean distance to the riparian zone in the Punatsangchhu River Basin ranges between 0 and 510 m. The darker blue represents areas closer to the river, and the lighter blue indicates areas farther from it. Areas near the river are usually at higher risk of flooding and related hazards, such as erosion and pollution (Narasayya, 2024).

Rainfall

The rainfall map for the riparian zones of the Punatsangchhu River Basin is shown in Figure 5k. Rainfall in the riparian zone of the Punatsangchhu River Basin ranges from 141.5 mm to 1828.59 mm. The darker brow in the lower region of the study area represents the high rainfall areas. Whereas the middle and upper region of the study area, indicated by blue color, reflects the higher rainfall areas.

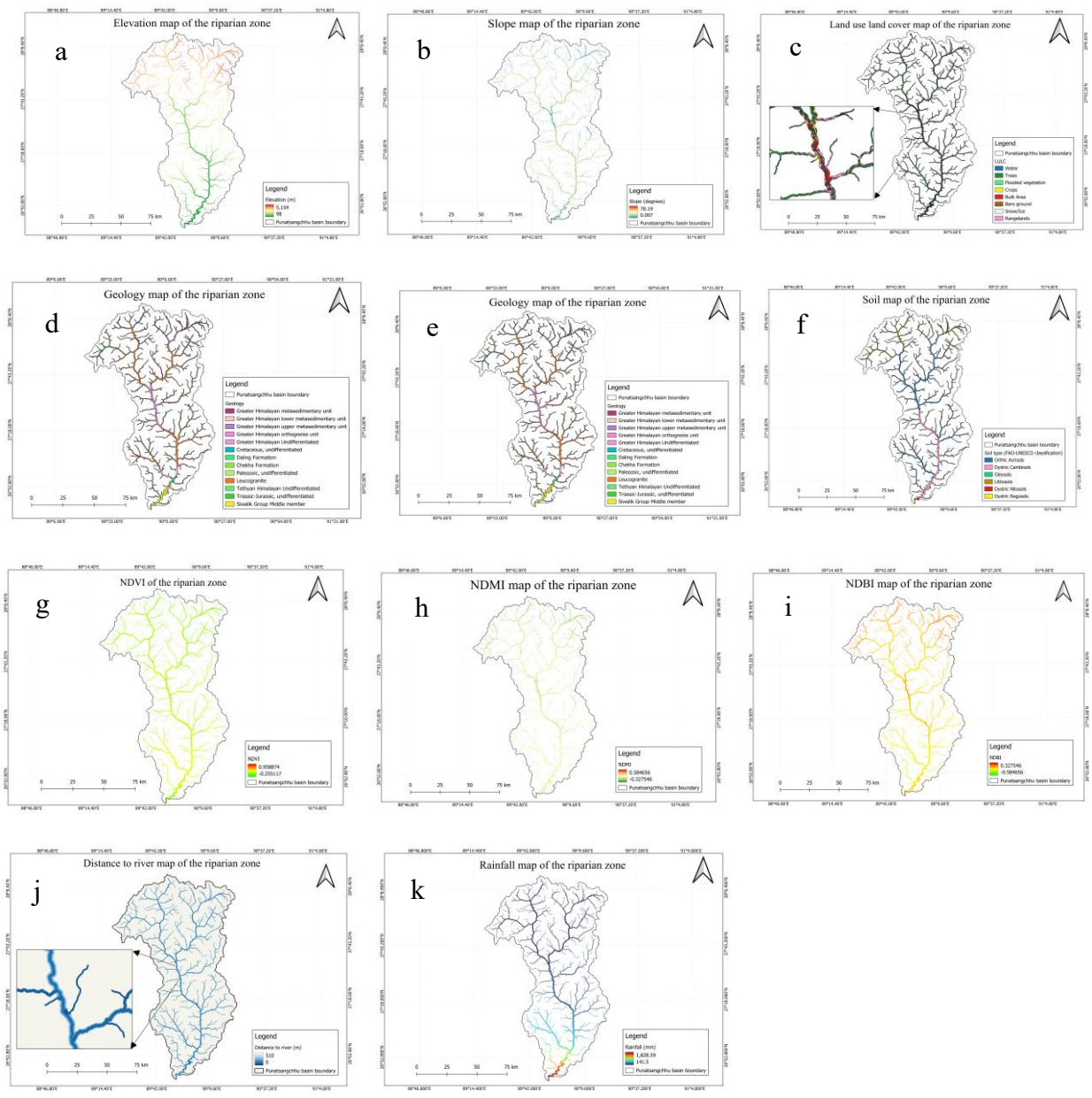


Figure 1: Conditioning factors of the riparian zone risk modeling

Identification of key drivers using Information Gain Ratio (InGR)

The results of the information gain ratio of the riparian zones in the Punatsangchhu River Basin are presented in Table 4. The results revealed that LULC is the most influential indicator of the riparian zone risk modeling, as indicated by the information gain ratio importance score of 0.165. The second most influential indicator is the geomorphology, with an information gain ratio importance score of 0.097, followed by elevation, with an information gain ratio importance score of 0.087. The details of the importance score for each variable are represented in Table 4.

Table 4: The table shows the importance value for all the variables derived from Information Gain Ratio.

No	Variables	Importance
1	LULC	0.165
2	Geomorphology	0.095
3	Elevation	0.087
4	Slope	0.079
5	Geology	0.052
6	NDBI	0.045
7	NDMI	0.043
8	Soil	0.031
9	NDVI	0.024
10	Rainfall	0.020
11	Distance to river	0.009

Risk assessment using machine learning algorithms

The riparian zone risk maps generated using RF and SVM algorithms were presented in Figure 6 and Figure 7, respectively. The outputs of both RF and SVM models are classified into five risk zones: very low (0.00 – 0.20), low (0.20 – 0.40), moderate (0.40 – 0.60), high (0.60 – 0.80), and very high (0.80 – 1.00). The lower, middle, and higher regions within the study area, represented in red, are high-risk areas, and the middle region represents the lower-risk areas. In the RF model, 398.51 km² is predicted as a very low risk area, and 112.81 km² is predicted as a very high risk zone. The SVM model also predicted 399.51 km² as very low risk zones and 85.44 km² as a very high risk zone. The details of the area statistics for each machine learning algorithm are presented in Table 5.

Table 5: Area statistics of the riparian zone risk zone as predicted by machine learning algorithms.

Riparian risk assessment		Very Low	Low	Moderate	High	Very High
SVM	Area (Km²)	399.51	119.29	117.79	80.21	85.44
	Area (%)	50%	15%	14%	10%	11%
	Pixel count	443902.0	132539.00	130879.0	89121.00	94931.00
RF	Area (Km²)	398.51	107.85	75.94	107.13	112.81
	Area (%)	49%	13%	9%	13%	14%
	Pixel count	442792.0	119833.0	84377.0	119028.0	125342.0

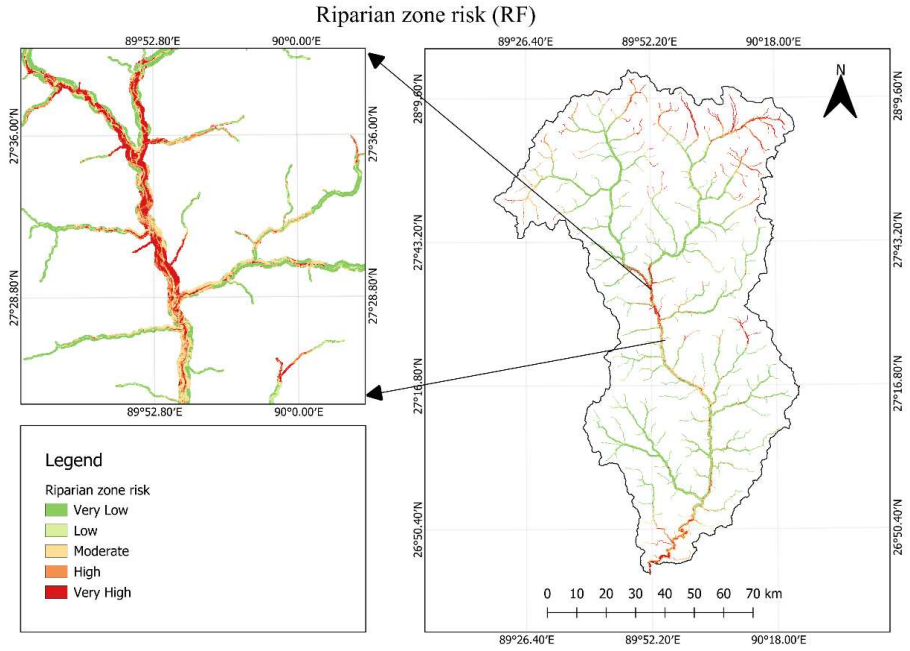


Figure 6: The map shows the predicted riparian zone risk class by the RF algorithm

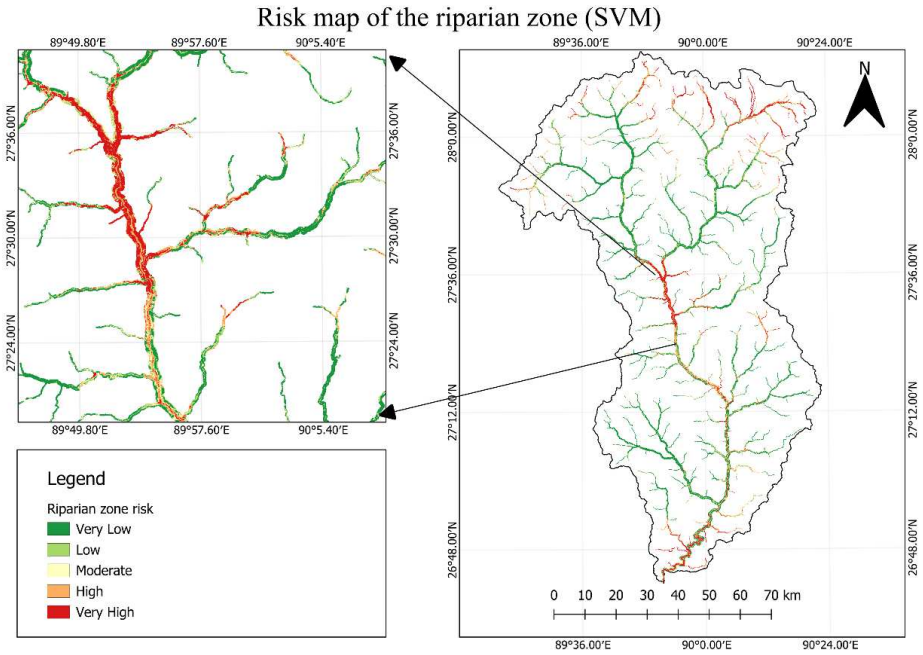


Figure 7: The map shows the predicted riparian zone risk class by the SVM algorithm

Model evaluation

The model validation map of the riparian zones in the Punatsangchhu River Basin is presented in Figure 8. In the present study, the riparian zone risk model was validated for both RF and SVM algorithms using the area under the curve (AUC) value of the receiver operating characteristic curve (ROC). To validate the model using the AUC value, the model's sensitivity was plotted on

the y-axis and specificity on the x-axis, using the 1% cumulative interval. The AUC values of the ROC curves for the riparian zone risk model using RF and SVM are 0.971 and 0.942, respectively. The AUC values for both machine learning algorithms suggest good model performance. However, the RF has shown better predictive accuracy than the SVM (Figure 8).

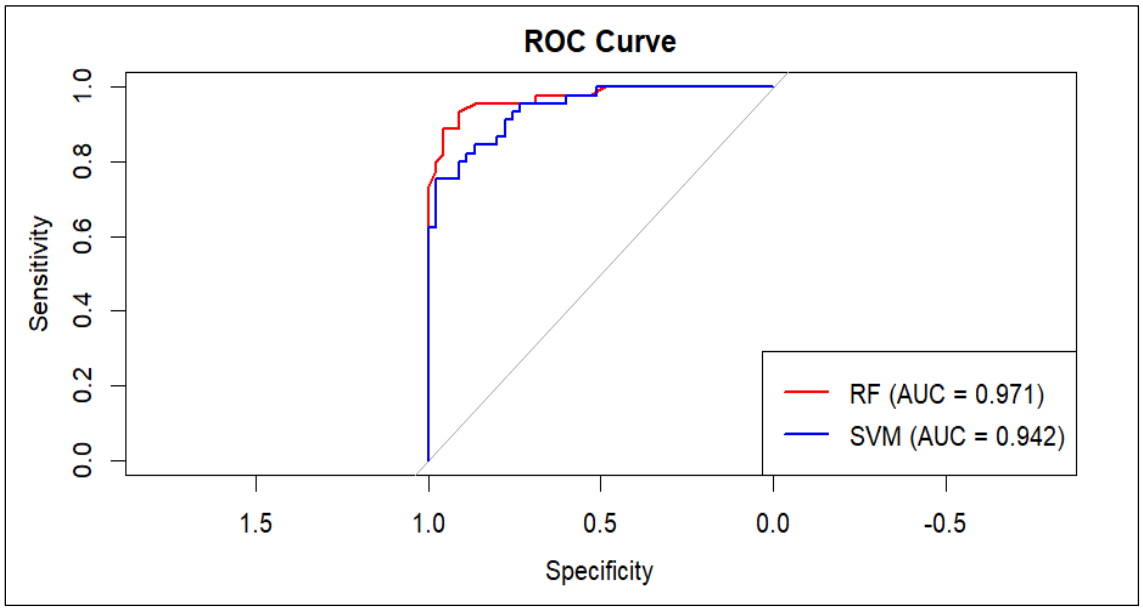


Figure 8: ROC curve of the riparian zone risk model using RF (red) and SVM (blue) algorithms.

Discussion

This study identifies vulnerable areas in the riparian zone of the Punatsangchhu River basin in western Bhutan. Such risk assessment studies can help us formulate strategies to reduce damage and fatalities (Zhu et al., 2025). Additionally, it helps predict and identify susceptible landscapes that can cause damage and loss of life and property (Islam et al., 2021a). As indicated in the results section, a diverse array of indicators influences the riparian zone's vulnerability, leading to risk. This study analyzed both natural and anthropogenic factors for the riparian zone risk assessment. The findings suggest that LULC is the most influential driver of the riparian zone risk assessment, followed by geomorphology, elevation, and geology, as indicated by the high information gain ratio score.

This shows the dominant role of LULC in riparian zone risk modeling, as it indicates modifications in riparian areas that can alter the degree of riparian vegetation fragmentation, degrade streamside habitats, and affect biological communities (Yirigui et al., 2019). Similar findings were reported by several studies that riparian condition depends heavily on prevailing land-use patterns, which suggests that human activities threaten riparian habitats (Olokeogun & Kumar, 2022). Moreover, Okeke et al. (2022) reported that bank erosion and accretion were higher due to rapid land-use changes in the Nkisi River Watershed, Nigeria. In addition, these findings are supported by Hanna

et al. (2019), who reported that the ecosystem services and ecosystem health of the stream were higher in the watershed's intact forest than in the disturbed forest.

The high InGR score of geomorphology, elevation, and slope signals an influential role of these factors in riparian zone risk modeling. Elevation and slopes play a crucial role in determining runoff, infiltration rates, and sediment dynamics, which directly affect soil moisture and biological communities in a hydrological unit (Breinl & Lun, 2021). Similar findings were reported that elevation is the most influential factor in the ecological risk assessment studies (Hou et al., 2020; Karimian et al., 2022; Cui et al., 2022). Likewise, geomorphology lies at the center of riparian zone risk assessment. It controls the riparian ecosystem's sensitivity and resilience to disturbance, shaping the riparian vegetation communities (Naiman & Décamps, 1997).

Moreover, the present study identified high-vulnerability areas within the riparian zone of the Punatsangchhu River Basin. The findings show the high-risk areas are concentrated in the middle part of the riparian zone of the Punatsangchhu River Basin. This indicates the impacts of land-use and land-cover changes resulting from hydropower projects (PHPA I and PHPA II), urban settlements (Bajo and Khuruthang towns), and agricultural expansion (Wangdi, 2014). Studies on ecological risk assessment also reported similar results, indicating that human activities, such as land-use and land-cover change and agricultural expansion, are directly linked to the vulnerability of the riparian ecosystem (Olokeogun & Kumar, 2022; Islam et al., 2021a). For instance, Olokeogun and Kumar (2022) revealed that urbanization has significantly impacted the condition of the riparian zone.

Additionally, highly elevated areas in the upper region of the basin showed a concentration of high risk areas. This is also consistent with existing studies (Cui et al., 2022; Wang et al., 2020). The upper parts of basin areas often have high altitudes and steep slopes, which show a significant positive correlation with ecological risk, which may explain the high-risk areas in the upper part of the Punatsangchhu River Basin (Wang et al., 2020). These high risk areas in the riparian zone have crucial conservation implications beyond the riparian risk zonation. Riparian zones within the Punatsangchhu River Basin are a critical habitat for the critically endangered White-bellied Heron. The concentration of high ecological risk in these areas may affect the habitat and foraging ground of the White-bellied Heron, as studies have reported that it prefers undisturbed areas (Wangdi, 2014; Maheswaran et al., 2021).

Although the present study produced good results, it acknowledges several limitations. In this study, the binary-labeled data used to train the ML algorithms were obtained from integrated remote sensing and GIS operations adapted from landscape ecology (Islam et al., 2021a). These operations would have been better if they had been field-validated to understand the ground reality of riparian conditions in the Punatsangchhu River Basin. Moreover, field data would improve the predictive accuracy of ML algorithms in risk modeling. This study employed two ML algorithms;

future studies can use multiple algorithms, and ensemble their outputs could produce a better model with higher accuracy (Islam et al., 2021b).

In addition, this study produced only a current risk map of the riparian zone, but future studies can forecast future risks using climate and LULC change scenarios (Zhu et al., 2025). For instance, Zhu et al. (2025) used the PLUS model to predict future riparian zone risk under land-use scenarios. In the present study, key influential factors of riparian risk vulnerability are assessed using a feature selection approach, namely, information gain ratio (InGR), and all the factors are retained for risk modeling. However, the riparian zone risk modeling would have been affected by the spatial autocorrelation of the predictor variables. Thus, this study recommends checking multicollinearity among the predictors using Pearson correlation and retaining only one predictor from each pair with an absolute Pearson correlation coefficient less than 0.8. The present study used only indicators readily extracted from remote sensing. However, this study recommends integrating other relevant indicators of riparian zone vulnerability, such as pollutant discharge intensity and population density (Islam et al., 2021a; Zhu et al., 2025). Moreover, variable-width buffering of stream data was used to delineate the riparian zone, but this approach does not capture the actual riparian extent. Thus, this study also recommends using robust techniques such as fuzzy logic and machine learning algorithms (Clerici et al., 2013, 2014; Weissteiner et al., 2016; Betz et al., 2018; Salo & Theobald, 2016).

Moreover, this study also identified five risk classes in the riparian zone of the Punatsangchhu River Basin. Although very high-risk areas occupy only 11% and 14%, respectively, as predicted by SVM and RF. The high-risk areas predicted in the middle, lower, and upper regions of the basin are sensitive, and it is recommended that risk response measures be formulated to mitigate loss of life and property damage. For instance, these regions should be prioritized for riparian buffer development and for regulated land-use practices. These findings would provide crucial information to formulate an efficient plan for conserving riparian areas to support future developmental activities, such as hydropower development, within the river basin. Moreover, these findings could also support competent authorities involved in managing and protecting the riparian zone in monitoring its condition and initiating restoration in the high-risk and very high-risk areas identified by the riparian risk model. Moreover, these findings can help competent authorities guide restoration and remediation in high and very high risk areas. Therefore, this study plays a significant role in the management of the riparian fringe in the Punatsangchhu River Basin.

Conclusion

In conclusion, this study predicted the riparian zone risk within the Punatsangchhu River Basin. The low-risk class in the riparian zone is the most dominant, with 50% and 49% predicted by SVM and RF, respectively. The following conclusions can be drawn from the above findings. This study successfully delineated the riparian zone using variable-width buffering of stream data in the Punatsangchhu River Basin. From the diverse array of indicators used in the current study, land use and land cover, and geomorphology are the most influential factors driving riparian zone risk.

The RF algorithms outperformed the SVM in terms of predicting riparian zone risk vulnerability. The AUC values are 0.97 and 0.94, respectively. The high-risk areas within the riparian zone are concentrated in the middle, lower, and upper parts of the Punatsangchhu River Basin. A very high-risk riparian zone accounts for only 11% and 14% according to SVM and RF, respectively. This study recommends conducting ecological risk assessments.

References

Apan AA, Raine SR, Paterson MS (2002) Mapping and analysis of changes in the riparian landscape structure of the Lockyer Valley catchment, Queensland, Australia. Landsc Urban Plan 59(1):43–57. https://doi.org/10.1016/S0169-2046(01)00246-8.

Ashcroft MB (2010) Identifying refugia from climate change. J Biogeogr 37(8):1407–1413. https://doi.org/10.1111/j.1365-2699.2010.02300.x.

Betz F, Lauermann M, Cyffka B (2018) Delineation of the riparian zone in data-scarce regions using fuzzy membership functions: An evaluation based on the case of the Naryn River in Kyrgyzstan. Geomorphology 306(2018):170–181. https://doi.org/10.1016/j.geomorph.2018.01.024.

Bhatti SS, Tripathi NK (2014) Built-up area extraction using Landsat 8 OLI imagery. GISci Remote Sens 51(4):445–467. https://doi.org/10.1080/15481603.2014.939539.

Bottaro C, Finizio M, Innangi M, Varricchione M, Carranza ML, Sona G (2025) Ecological Insights from Above: Linking Habitat-Level NDVI Patterns with NDMI, LST and Elevation in a Small Mediterranean City (Italy). Land 15(1):57

Breinl K, Lun D (2021) Understanding the relationship between rainfall and flood probabilities through combined intensity-duration-frequency analysis. J Hydrol 602:126759. https://doi.org/10.1016/j.jhydrol.2021.126759.

Burger B, Reich P, Cavagnaro TR (2010) Trajectories of change: riparian vegetation and soil conditions following livestock removal and replanting. Austral Ecol 35(8):980–987. https://doi.org/10.1111/j.1442-9993.2010.02112.

Carpenter SR, Stanley EH, Vander Zanden MJ (2011) State of the World's Freshwater Ecosystems: Physical, Chemical, and Biological Changes. Annu Rev Environ Resour 36(1):75–99. https://doi.org/10.1146/annurev-environ-021810-094524.

Kitzmann N, Caesar L, Sakschewski B, Rockström J, Andersen L, Bechthold M, Wunderling N (2025) *Planetary Health Check 2025: A scientific assessment of the state of the planet.* Potsdam: Potsdam Institute for Climate Impact Research.

Clerici N, Weissteiner CJ, Paracchini ML, Boschetti L, Baraldi A, Strobl P (2013) Pan-European distribution modelling of stream riparian zones based on multi-source Earth Observation data. Ecol Indic 24(2013): 211–223. https://doi.org/10.1016/j.ecolind.2012.06.002.

Clerici N, Paracchini M L, Maes J (2014) Land-cover change dynamics and insights into ecosystem services in European stream riparian zones. Ecohydrol Hydrobiol 14(2):107–120. https://doi.org/10.1016/j.ecohyd.2014.01.002.

Correll DL, Jordan TE, Weller DE (1992) Nutrient Flux in a Landscape: Effects of Coastal Land Use and Terrestrial Community Mosaic on Nutrient Transport to Coastal Waters Watersheds and Coastal Waters. Estuaries 15(4):431–442

Cui B, Zhang Y, Wang Z, Gu C, Liu L, Rai MK (2022) Ecological Risk Assessment of Transboundary Region Based Basin, Himalayas. Land 11(5):638

Dodds WK, Perkin JS, Gerken JE (2013) Human Impact on Freshwater Ecosystem Services: A Global Perspective. Environ Sci Technol 47(16):9061-9068

Food and Agriculture Organization (1974) Soil map of the world. UNESCO.

Florim I, Albert B, Shpejtim B (2021) Measuring UHI using Landsat 8 OLI and TIRS data with NDVI and NDBI in Municipality of Prishtina. Disaster Adv 14(11):25–36

Fu B, Burgher I (2015) Riparian vegetation NDVI dynamics and its relationship with climate, surface water and groundwater. J Arid Environ 113:59–68. https://doi.org/10.1016/j.jaridenv.2014.09.010.

Funk A, Martínez-lópez J, Borgwardt F, Trauner D, Bagstad KJ, Balbi S, Magrach A, Villa F, Hein T (2019). Identification of conservation and restoration priority areas in the Danube River based on the multi-functionality of river-floodplain systems. Sci Total Environ 654:763–777. https://doi.org/10.1016/j.scitotenv.2018.10.322.

Garcin Y, Schefuß E, Dargie GC, Hawthorne D, Lawson IT, Sebag D, Biddulph GE, Crezee B, Bocko YE, Ifo SA, Mampouya Wenina YE (2022) Hydroclimatic vulnerability of peat carbon in the central Congo Basin. Nature 612(7939):277-282. https://doi.org/10.1038/s41586-022-05389-3.

Grafton RQ, Pittock J, Williams J, Jiang Q, Possingham H, Quiggin J (2014) Water Planning and Hydro-Climatic Change in the Murray-Darling Basin , Australia. Ambio 43(8):1082–1092. https://doi.org/10.1007/s13280-014-0495-x.

Gregory SV, Swanson FJ, McKee WA, Cummins KW (1991) An Ecosystem Perspective of

Riparian Zones. *BioScience* 41(8):540–551. https://doi.org/10.2307/1311607.

Gurung DB, Dorji U, Dorjee S (2024) Hydropower and Aquatic Ecosystems: A Study of Macroinvertebrate Diversity. Int J Innov Res Sci Eng Technol 13(9):15901–15908. https://doi.org/10.15680/IJIRSET.2024.1309001

Hanna DEL, Hearne CR, Bennett EM (2019) Effects of land use, cover, and protection on stream and riparian ecosystem services and biodiversity. Conserv Biol 34(1):244–255. https://doi.org/10.1111/cobi.13348

He F, Zarfl C, Tockner K, Olden JD, Campos Z, Muniz F, Svenning JC, Jähnig SC (2024) Hydropower impacts on riverine biodiversity. Nat Rev Earth Environ 5(11):755–772. https://doi.org/10.1038/s43017-024-00596-0

Hou M, Ge J, Gao J, Meng B, Liu J, Feng Q, Liang T (2020) Ecological Risk Assessment and Impact Factor Analysis of Alpine Wetland Ecosystem Based on LUCC and Boosted Regression Tree on the Zoige. Remote Sens 12(368):1–22.

Hultine KR, Bush SE, Ehleringer JR (2010) Ecophysiology of riparian cottonwood and willow before, during, and after two years of soil water removal. Ecol Appl 20(2): 347–361.

Islam ARMT, Talukdar S, Mahato S, Ziaul S, Eibek KU, Akhter S, Pham QB, Mohammadi B, Karimi F, Nguyen TTL (2021a) Machine learning algorithm-based risk assessment of riparian wetlands in Padma River Basin of Northwest Bangladesh. Environ Sci Pollut Res 28(26):34450–34471.

Islam ARMT, Talukdar S, Mahato S, Kundu S, Eibek KU, Pham QB, Kuriqi A, Nguyen TTL (2021b). Flood susceptibility modelling using advanced ensemble machine learning models. Geosci Front 12(3):101075 https://doi.org/10.1016/j.gsf.2020.09.006

Indian Space Research Organization (2010) Manual for National Geomorphological and Lineament Mapping on 1:50,000 scale. ISRO.

Jamtsho K, Lund MA, Blake D, Van Etten E (2024) Microplastic Pollution in Riparian Soils of the Rapidly Growing City of Thimphu, Bhutan. Water, Air, and Soil Pollut 235(11):1–16. https://doi.org/10.1007/s11270-024-07536-0

Jamtsho T, Wangchuk P, Yeshi K, Tobgay, Sridith K (2021) Riparian plant species of Sherichhu River in Eastern Bhutan: their diversity, distribution, and ethnobotanical uses. Trop Ecol 62(4):563–579. https://doi.org/10.1007/s42965-021-00173-2

Johansen K, Phinn S (2006) Mapping Structural Parameters and Species Composition of

Riparian Vegetation Using IKONOS and Landsat ETM+ Data in Australian Tropical Savannahs. Photogramm Eng Remote Sens 72(1):71–80.

Jones KB, Slonecker ET, Nash MS, Neale AC, Wade TG, Hamann S (2010) Riparian habitat changes across the continental United States (1972-2003) and potential implications for sustaining ecosystem services. Landsc Ecol 25(8):1261–1275. https://doi.org/10.1007/s10980-010-9510-1.

Kaintura D, Dasgupta S, Chauhan DS (2024) Impacts of hydropower-induced flow alterations on composition and diversity of riparian vegetation in the Western Himalayas: A case study in Uttarakhand, India. J Mt Sci 21(4):1272–1286. https://doi.org/10.1007/s11629-024-8606-z

Karimian H, Zou W, Chen Y, Xia J, Wang Z (2022) Landscape ecological risk assessment and driving factor analysis in Dongjiang river watershed. Chemosphere 307:135835. https://doi.org/10.1016/j.chemosphere.2022.135835.

Lesmeister C (2017) Mastering Machine Learning with R. Packt Publishing.

Lhundup K, Dorji U (2018) Macro-invertebrate Diversity and its Relationship with Environmental Variables in Adha Lake between Monsoon and Post-monsoon Seasons. Bhutan J Nat Res Dev 5(1):13–24. https://doi.org/10.17102/cnr.2018.02.

Li J, Hu D, Wang Y, Chu J, Yin H, Ma M (2024) Study of identification and simulation of ecological zoning through integration of landscape ecological risk and ecosystem service value. Sustain Cities Soc 107:105442. https://doi.org/10.1016/j.scs.2024.105442.

Lungten L, Acharja IP, Tobgay T, Phuntsho T, Lhendup T (2023) Diversity of benthic macroinvertebrates in White-bellied Heron landscape Punatsangchhu and Mangdechhu River, Bhutan. Int J Fauna Biol Stud 10(4): 09–17. https://doi.org/10.22271/23940522.2023.v10.i4a.967.

Maheswaran G, Kumar L, Sekhar H (2021) White-bellied heron a species on the verge of extinction: Ensemble model reveals loss of habitats and resultant prolonged isolation driving the species to extinction. Ecol Inform 64:101383. https://doi.org/10.1016/j.ecoinf.2021.101383.

Majumdar A, Avishek K (2023) Riparian Zone Assessment and Management: an Integrated Review Using Geospatial Technology. Water, Air, Soil Pollut 234(5). https://doi.org/10.1007/s11270-023-06329-1

Maraseni TN, Mitchell C (2016) An assessment of carbon sequestration potential of riparian

zone of Condamine Catchment , Queensland , Australia. Land Use Policy 54:139–146. https://doi.org/10.1016/j.landusepol.2016.02.013

Mcquarrie N, Long SP, Tobgay T, Nesbit JN, Gehrels G, Ducea MN (2013). Documenting basin scale, geometry and provenance through detrital geochemical data : Lessons from the Neoproterozoic to Ordovician Lesser, Greater, and Tethyan Himalayan strata of Bhutan. Gondwana Res 23(4):1491–1510. https://doi.org/10.1016/j.gr.2012.09.002

Millennium Ecosystem Assessment (2005) *Ecosystems and Human Well-Being*. World resources institute.

Naiman RJ, Décamps H (1997) The ecology of interfaces: Riparian zones. Annu Rev Ecol Syst 28(1):621–658. https://doi.org/10.1146/annurev.ecolsys.28.1.621

Narasayya K (2024) An Innovative Method for Flood Susceptibility Mapping Integrated MCDM-WOA Model with Geospatial Techniques and Remote Sensing Data – An ArcGIS based Approach. Int J Innov Res Sci Eng Technol 13(10). https://doi.org/10.15680/IJIRSET.2024.1310034

Narumalani S, Zhou Y, Jensen JR (1997) Application of remote sensing and geographic information systems to the delineation and analysis of riparian buffer zones. Aquat Bot 58(3–4):393–409. https://doi.org/10.1016/S0304-3770(97)00048-X

Okeke CAU, Uno J, Academe S, Emenike PC, Abam TKS, Omole DO (2022) An integrated assessment of land use impact, riparian vegetation and lithologic variation on streambank stability in a peri-urban watershed (Nigeria). Sci Rep 12(1):10989. https://doi.org/10.1038/s41598-022-15008-w

Olokeogun OS, Kumar M (2022) Indicator-based vulnerability assessment of riparian zones in Nigeria's Ibadan region due to urban settlement pressure. Environ Chall 7:100501. https://doi.org/10.1016/j.envc.2022.100501

Olokeogun OS, Kumar M (2020) An indicator based approach for assessing the vulnerability of riparian ecosystem under the influence of urbanization in the Indian Himalayan city, Dehradun. Ecol Indic 119:106796. https://doi.org/10.1016/j.ecolind.2020.106796

Salo JA, Theobald DM (2016). A multi-scale, hierarchical model to map riparian zones. River Res Appl 32(8):1709–1720. https://doi.org/10.1002/rra

Intergovernmental Science-Policy Platform on Biodiversity and Ecosystem Services (2019) Global Assessment Report on Biodiversity and Ecosystem Services. IPBES Secretariat.

Thukten K (2024) Plant species diversity along altitudinal gradient of Chamkhar River Basin, Central Bhutan. Asian J For 8(1):81–87. https://doi.org/10.13057/asianjfor/r080108.

Toole PO, Chambers JM, Bell RW (2018) Understanding the characteristics of riparian zones in low relief, sandy catchments that affect their nutrient removal potential. Agric Ecosyst Environ. 258:182–196. https://doi.org/10.1016/j.agee.2018.02.020

United States Environmental Protection Agency (1998) Guidelines for Ecological Risk Assessment, *63*. USEPA

Wang B, Ding M, Li S, Liu L, Ai J (2020) Assessment of landscape ecological risk for a cross-border basin: A case study of the Koshi River Basin, central Himalayas. Ecol Indic 117:106621. https://doi.org/10.1016/j.ecolind.2020.106621

Wang L, Liu H (2007) An efficient method for identifying and filling surface depressions in digital elevation models for hydrologic analysis and modelling. Int J Geogr Inf Sci 20(2):193–213. https://doi.org/10.1080/13658810500433453

Wangdi T (2014) Landuse change effect on habitat and White-bellied Heron population by hydropower project along Punatsangchu. (Bachelor's thesis College of Natural Resources), Royal University of Bhutan, Lobesa, Bhutan.

Weissteiner CJ, Ickerott M, Ott H, Probeck M, Ramminger G, Clerici N, Dufourmont H, de Sousa AMR (2016) Europe's green arteries-A continental dataset of riparian zones. Remote Sens 8(11):1–27. https://doi.org/10.3390/rs8110925.

Whitehead PG, Wilby RL, Battarbee RW, Kernan M, Wade AJ (2009) A review of the potential impacts of climate change on surface water quality. Hydrol Sci J 54(1):101–23. https://doi.org/10.1623/hysj.54.1.101

Yirigui Y, Lee SW, Nejadhashemi AP, Herman MR, Lee JW (2019) Relationships between riparian forest fragmentation and biological indicators of streams. Sustainability 11(10):1–24. https://doi.org/10.3390/su11102870

Zhang X, Ci X, Hu J, Bai Y, Thornhill AH (2023) Riparian areas as a conservation priority under climate change. Sci Total Environ 858:159879. https://doi.org/10.1016/j.scitotenv.2022.159879

Zhu Z, Zhang C, Lu Y, Ye J, Fang G, Sun C (2025) Ecological risk assessment and prediction of riparian zones in the Jiangsu section of the Yangtze River from a spatiotemporal perspective. Ecol Indic 174:113492. https://doi.org/10.1016/j.ecolind.2025.113492.

Acknowledgements

The authors sincerely thank the School of Ecology and Environment Studies, Nalanda University, Rajgir, India, for providing academic support. The authors also acknowledge all the individuals who assisted during data collection and provided valuable support throughout this research.

Funding

This research received no specific grant from any funding agency in the public, commercial, or not-for-profit sectors.

Authors' Contributions

Asish Subba conceived the study, collected and analyzed the data, prepared the figures and tables, and drafted the manuscript. Dr. Satyanarayan Shashtri supervised the research, provided scientific guidance throughout the study, critically reviewed the manuscript, and contributed to the interpretation of the results. Both authors read and approved the final manuscript.

Ethical Approval

This study did not involve human participants or experimental manipulation of animals. Ethical approval was therefore not required.

Consent to Participate

Not applicable.

Consent to Publish

All authors have read and approved the final manuscript and consent to its publication.

Competing Interests

The authors declare that they have no competing interests.

Data Availability Statement

The datasets generated and/or analyzed during the current study are available from the corresponding author upon reasonable request.